Fusion Technology

ISSN: 0748-1896 (Print) (Online) Journal homepage: http://www.tandfonline.com/loi/ufst19

ITER Divertor Research and Development Activities

D. Driemeyer, D. Bowers, J. Davis, D. Kubik, H. Mantz, M. McSmith, T. Rigney, C. Baxi, L. Sevier, M. Carelli, L. Green, D. Ruzic, D. Hayden, M. Gabler & J. Yuen

To cite this article: D. Driemeyer, D. Bowers, J. Davis, D. Kubik, H. Mantz, M. McSmith, T. Rigney, C. Baxi, L. Sevier, M. Carelli, L. Green, D. Ruzic, D. Hayden, M. Gabler & J. Yuen (1994) ITER Divertor Research and Development Activities, Fusion Technology, 26:3P2, 603-610, DOI: 10.13182/FST94-A40223

To link to this article: https://doi.org/10.13182/FST94-A40223

Published online: 10 Aug 2017.

ITER DIVERTOR RESEARCH AND DEVELOPMENT ACTIVITIES*

D. Driemeyer, D. Bowers, J. Davis, D. Kubik, H. Mantz, M. McSmith, T. Rigney
McDonnell Douglas Aerospace, P.O. Box 516, St. Louis, MO 63166-0516

C. Baxi, L. Sevier
General Atomics, P.O. Box 85608, San Diego, CA 92186-1194

M. Carelli, L. Green
Westinghouse Science and Technologies Center, 1310 Beulah Rd., Pittsburgh, PA 15235

D. Ruzic, D. Hayden
University of Illinois, Dept. of Nucl. Eng., 103 S. Goowdin Ave., Urbana, IL 61801-2984

M. Gabler, J. Yuen
Rockwell International Corporation, Rocketdyne Division, 6633 Canoga Ave., Canoga Park, CA 91303

ABSTRACT

One of the key challenges in designing the next generation tokamaks is the development of plasma facing components (PFC's) that can withstand the severe environmental conditions at the plasma edge. The most intensely loaded element of the PFC's is the divertor. The divertor must handle high fluxes of energetic plasma particles and electromagnetic radiation without excessive impurity build-up in the plasma core. It must also remove helium ash while recirculating a large fraction of the unburned hydrogen fuel so that vacuum pumping requirements are not excessive. The gas-dynamic mode of divertor operation proposed for ITER expands the divertor design window to include several alternate heat sink and armor materials that were not feasible for the previous high recycling divertor approach. In particular, beryllium armor can now be considered with copper, niobium or vanadium structural materials cooled by liquid metal or possibly helium in addition to water.

This paper presents some of the results achieved under ongoing ITER Plasma Facing Components research and development tasks. The overall effort involves U.S. industry, universities and national laboratories and is directed towards developing and/or testing: (1) ductile beryllium and beryllium joining techniques; (2) prototype divertor component design, fabrication and testing; (3) fiber-reinforced composites for beryllium and carbon; (4) beryllium plasma spray processes; (5) compliant layers for PFC armor attachment; (6) sacrificial armor layers for the divertor end-plates; and (7) tritium permeation and inventory in proposed PFC materials and components. The paper focuses on work being conducted by the industrial support team consisting of McDonnell Douglas Aerospace, Ebasco, General Atomics, Rocketdyne, University of Illinois and Westinghouse.

I. ITER DIVERTOR DESIGN REQUIREMENTS

The nominal power during the ITER burn is 1.5 GW with an energy confinement time of 4.5 s. All 300 MW of alpha power effectively heats the plasma, so the stored thermal energy is 1.35 GJ. The divertor has to handle this normal exhaust power as well as abnormal exhaust of large fractions of the plasma stored energy during power excursions, sawteeth collapses, ELM's and disruptions. The divertor surface must also consist of a low atomic number material that provides a reasonable lifetime (~1 year) in the presence of sputtering erosion and surface ablation during off-normal events. Due to uncertainties in the power distribution between the divertor and first wall, the design assumes that the divertor must be capable of dissipating 80% of the alpha plus external heating power. To manage this heat load, the proposed approach for the single-null ITER divertor is therefore to exhaust the scrape-off power perpendicular to the field lines using atomic and molecular processes in a high-density, neutral-gas target formed within the divertor channels[1]. This increases the target surface area to ~400 m^2 and lowers the design heat flux to 5 MW/m^2, including allowances for expected peaking factors and power excursions. This reduction in surface heating provides a larger design window for the divertor and promises improved reliability and longer lifetimes.

* Work supported by the Office of Fusion Energy, U.S. Department of Energy under subcontract AC3013 with Sandia National Laboratories, U.S. DOE Contract No. DE-AC04-76DP00789.

Figure 1 shows the resulting divertor design concept. The design consists of five main elements: (1) a central dome structure that shadows the private flux sidewalls and, together with the toroidal limiters/baffles, restricts neutral flow back into the main plasma chamber; (2) toroidal limiters/baffles that shadow the inner and outer sidewalls; (3) vanes that handle the high power sidewall exhaust yet form an open structure for neutral gas recycle and helium pumping; (4) sacrificial end plates that handle disruption loads and (5) a modular cassette structure that provides component support, coolant manifolding and shielding for the surrounding magnet field coils. The industrial team is currently supporting the ITER divertor development work in the following areas: (1) design trade studies and performance assessments of divertor element design concepts, (2) development of compliant thermal interface materials for attaching replaceable armor layers, and (3) design and fabrication of beryllium samples and sample holders for evaluating tritium permeation and retention in the upgraded Tritium Plasma Experiment facility.

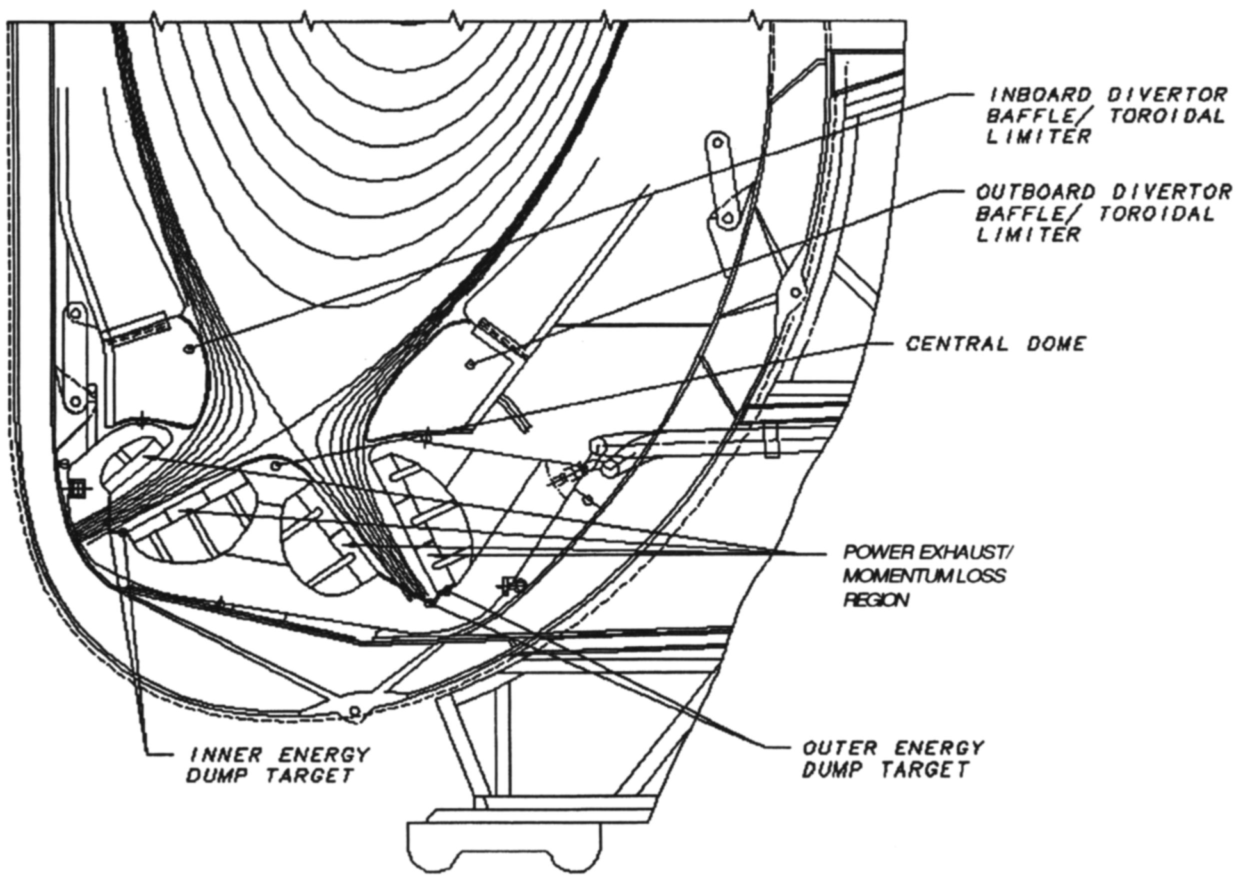

Figure 1. Cross-section through ITER divertor showing major design elements.

II. DIVERTOR DESIGN TRADE STUDIES AND PERFORMANCE ASSESSMENTS

In the first area, an extensive study of engineering and materials performance and fabrication constraints for the dynamic-gas-target divertor was conducted and documented during 1993[2]. Physics models of the dynamic gas divertor were developed and used to evaluate preliminary wall heating and erosion estimates. This information was used to assess compatibility and performance limitations for beryllium armor with copper, niobium and vanadium heatsink materials using water, helium or liquid metal coolants. Finally, research and development issues unique to the engineering design concepts applicable to the gas-dynamic mode of operation were identified and summarized in the report.

Gas-dynamic divertor modeling at the University of Illinois has continued in support of the design activity. The purpose of this work is to (1) provide the proper input for sputtering calculations and surface erosion/redeposition assessments, (2) determine surface heat loads on the divertor elements to support engineering design studies, (3) compare with fluid-code models of the divertor channel for validation purposes. The modeling uses the DEGAS Monte-Carlo neutral transport code[3] and includes molecules and wall reflections. Background plasma conditions and geometry are taken from two-dimensional PLANET fluid code[4] models of the ITER edge plasma that include recombination and develop a detached ionization front. Typical background plasma temperature profiles for a detached gaseous divertor solution are shown in Figure 2. Neutral sources for this solution are determined based on wall recycling and volumetric recombination effects.

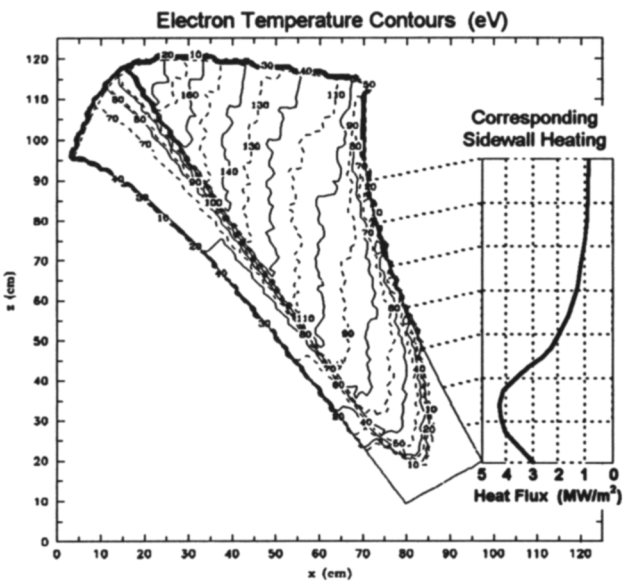

Figure 2. Typical background plasma conditions used for DEGAS initialization. The resulting sidewall heat distribution is also indicated.

A key element of this effort involves the evaluation of power and particle load distributions on the divertor channel surfaces. A DEGAS post-processor has been developed that calculates the radiative heat flux component based on predicted volumetric recombination rates. A typical sidewall heating profile along the outer divertor leg is included in Figure 2 for the nominal input power of 220 MW. This profile illustrates the peak that develops at the position of the ionization front. Note that the peak is within the 5 MW/m^2 guideline adopted for divertor engineering design and is mostly a result of radiative flux, not charge-exchange neutrals. This is encouraging because the present model does not include absorption and re-emission effects which are expected to lower the peak value. The most disturbing aspect of the edge modeling involves excessive armor erosion rates predicted at some locations along the sidewalls due to the low sputtering threshold for beryllium. This is discussed in more detail in Ref. 5 and ongoing work is attempting to refine the physics models and identify engineering changes that mitigate the problem.

The sidewall heat flux distribution shown in Figure 2 is being coupled with a view-factor analysis that includes the effect of reflections and re-emission to determine surface heat loads on a typical divertor vane. The geometry used in a two-dimensional version of this model is shown schematically in the insert block of Figure 3. This analysis assumed that the incident plasma heat flux was diffuse and that surface emissivity was not a function of temperature. The vane surface was divided into small elements and the computer code FACET[6] used to calculate view factors from the plasma source to each element representing the surface of the vane and to the gap between vanes at the bottom. Emissivity of gaps at the top and bottom of vanes was assumed to be 1.0. When the vane surface emissivity is 1.0, corresponding to zero reflectivity, view factors are adequate to calculate the heat flux distribution.

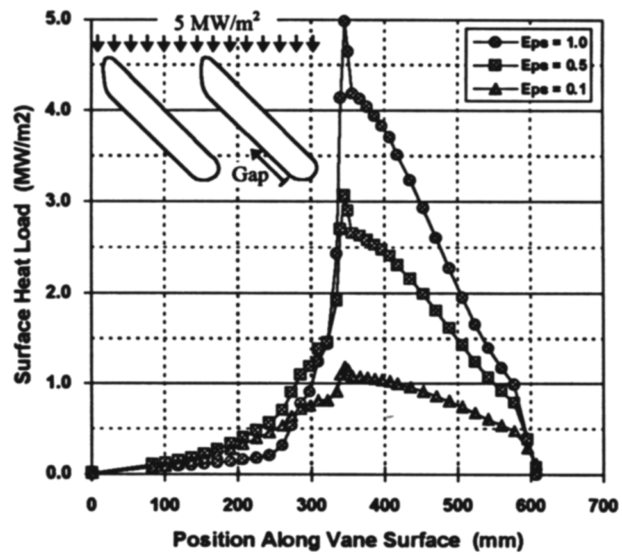

Figure 3. Heat flux distribution around divertor vane for three different emissivities. Insert shows divertor vane geometry used for view factor analysis.

If the surface of the vane is not black, the heat flux distribution is affected by reflections from surfaces. The resulting heat flux distribution can be calculated using the method developed by Hottel[7]. The method consists of solving the N simultaneous equations representing the radiosities of all surfaces. The General Atomics code HOTTELF[8] was used for these calculations. With the input of view factors, areas and emissivity of each of the surfaces, the code calculates exchange factors from each surface to all other surfaces. The exchange factors are used to calculate the heat fluxes on the surfaces. When the vane surfaces are gray, the net radiation heat flux from the plasma source is set to 5 MW/m^2.

Figure 3 shows the resulting heat flux around the vane as a function of emissivity. The heat flux is plotted versus distance around the vane, going in a clockwise direction from the origin indicated by the arrow in the insert. The peak heat flux and the net power flow to the vane decrease as emissivity drops because this allows a larger fraction of the power to escape through the gap between the vanes. For a surface emissivity of 1.0, the heat flux in the gap is about 0.7 MW/m^2, rising to about 1.2 MW/m^2 for an emissivity of 0.5. In practice the emissivity will be in this range which implies that the heat flux through the gap will be large enough to require cooling and protection for the vane support structure and exposed cassette surfaces. This could be avoided by modifying the vane shape or using smaller gaps between vanes. Ongoing work is assessing alternate shapes as well as vane thermal stresses resulting from three-dimensional surface heat fluxes.

More recent trade studies have focused on modifications to improve the performance of the baseline water-cooled sidewall vane concept indicated in Figure 1. Alternate flow channel configurations are being evaluated both from performance and fabrication standpoints. Based on the peaked surface heating profiles shown in Figure 3, coolant flow around the perimeter of the indicated vane cross-section should enhance performance. In fact, this flow geometry could be coupled with a local hypervapotron[9] around the leading edge of the vane to improve heat transfer and reduce the average flow velocity, hence pumping power. The benefits of this modification are being quantified in an ongoing trade study.

Another trade study is addressing concerns about flow instabilities that can develop in high-heat-flux components with many parallel flow channels. Instabilities can occur even when the bulk coolant is well subcooled because coolant channel surface temperatures can be above saturation locally due to hot spots, flow restrictions in one of the channels or other unforeseen events. Classical ways to prevent these instabilities include orificing, cross-flow promotion, surface heat transfer enhancement and limiting the number of channels. Westinghouse has proposed an open-channel concept[10] that avoids these parallel-flow problems. The concept is depicted in Figure 4 and could easily be adapted to the sidewall vanes. It consists of two parallel plates that are held in place by an array of pins or machined support segments that promote cross mixing. It can also include grids, such as those used in fission reactors, to suppress departure from nucleate boiling at hot spot locations. A mesh is located at the passage entrance to screen foreign objects, promote uniform flow distribution across the channel and provide form loss to prevent flow instabilities.

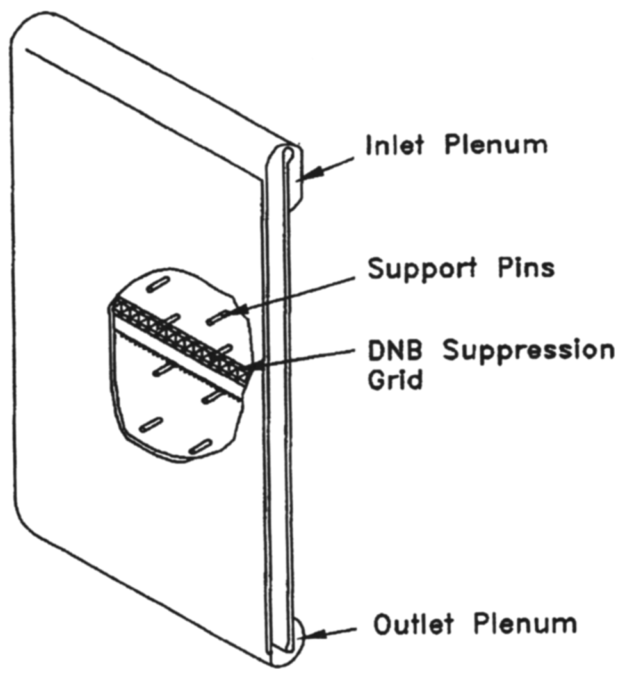

Figure 4. Schematic view of alternative open channel divertor vane design concept.

The results of a preliminary study of this approach are summarized in Ref. 10. Performance is comparable to the baseline design configuration, yet more robust due to the freedom from flow instabilities. The design is also more tolerant of bonding defects between the beryllium armor and copper structure due to the intimate coolant contact with the surface. Flaws up to 9 mm in size can be tolerated without exceeding the maximum beryllium surface temperature of 500°C. The attributes of this approach are thus particularly relevant to the peaked, yet unpredictable, heat fluxes expected in the ITER gas-dynamic divertor.

III. COMPLIANT LAYER DEVELOPMENT

A novel idea of compliant layer interfaces has been proposed for critical, frequently-replaced plasma-facing surfaces in ITER[11,12]. The compliant layer consists of a conventional soft solder alloy in the rheocast condition, possibly combined with a felt-metal carrier. The carrier would enhance the gap-filling capability and provide a framework to hold the compliant material in place during off-normal events. The solder alloy could be made to work in the solid state during normal operation and could be brought to the semi-solid state during armor replacement, simply by heating it slightly above the solidus temperature. Its function is to allow an efficient heat transfer between the replaceable armor and the permanent heat sink without building up excessive thermal stresses, as in conventional brazed joints. It would also promote in-situ armor replacement whenever needed, without disturbing the coolant system. Heat transfer is achieved without contact pressure and the reversible thixotropic properties of the rheocast material should provide mechanical stability of the layer in the semi-solid condition.

Five binary solder alloys were identified for preliminary evaluation as compliant layer materials. The alloys are listed in the top section of Table 1. These alloys are attractive because they (1) have a low vapor pressure, (2) have a relatively wide separation between solidus and liquidus temperature and (3) have a liquidus temperature below 350°C which eases in-situ refurbishment. They should function in the solid state during normal operating conditions for the water-cooled divertor currently being considered for ITER. One concern involves the proposed 300°C bake-out temperature. This suggests that the list be expanded to include higher temperature alloys such as those indicated in the lower section of Table 1. Candidate alloys from this list will be included in future evaluation studies.

Table 1. Candidate Compliant Layer Materials.

Solder Type	Solidus (°C)	Liquidus (°C)
90% In, 10% Ag	141	237
95% Bi, 5% Sn	134	251
90% Sn, 10% Ag	221	295
97% Sn, 3% Cu	227	300
99% Sn, 1% Ge	232	345
The following are of interest and will be evaluated		
90% Pb, 10%Sn	275	302
95% Pb, 5% Ag	305	364
90% Pb, 10% Ag	305	450
55% Ge, 45% Al	424	424
86% Al, 10% Si, 4% Cu	521	585

Initial results of the wetting studies are presented in Table 2. The preliminary work reported here considers only wetting studies on copper substrates. The wetting figure of merit is the angle formed at the solder/substrate interface. Wetting angles are determined from the diameter and height of the reflowed solder assuming a spherical cap geometry. Some samples were later cross-sectioned to compare the measured wetting angle with that resulting from the spherical cap model. There generally was good agreement between the two values as indicated in the table. Wetting angles were evaluated as a function of solder type, reflow environment and surface preparation technique for both the copper and solder.

Table 2 shows that wetting is generally good for all materials except the bismuth-based solder. The Bi/Sn sample had an obviously high wetting angle with flux and appeared to form a ball on the surface. It was therefore eliminated from further testing. Aside from this result, Table 2 shows no clear discriminators between the solder materials from a wetting perspective. With proper surface preparation, good wetting is achieved, even without flux, for all of the remaining solders. This is encouraging because it indicates that under controlled conditions, a good initial bond can be achieved without introducing flux residue into the vacuum environment. The remaining solders will thus be subjected to further studies including aging at expected 300°C operating temperatures to evaluate solder diffusion into the copper substrate, and interface void content investigations as a function of thermal cycling.

Table 2. Summary of Copper Wetting Studies with Candidate Solder Alloys.

Solder Type*	Copper Preparation Acid Etch	Process Environment	Process Temp °C	Wetting Angle Meas Deg	Wetting Angle Calc Deg
In90/Ag10	50/50 Nitric	Vacuum	398	10-12	8.1
Sn90/Ag10	HCl/Nitric	Vacuum	417	None	7.5
Sn99/Ge1	HCl/Nitric	Vacuum	467	None	7.1
Sn97/Cu3	50/50 Nitric	Vacuum	450	9	9.3
Sn97/Cu3	HCl/Nitric	Vacuum	425	None	11.5
In90/Ag10	50/50 Nitric	Flux/Argon	271	5-7	5.9
Sn90/Ag10	50/50 Nitric	Flux/Argon	406	5-7	8.0
Sn99/Ge1	50/50 Nitric	Flux/Argon	456	None	12.1
Sn97/Cu3	HCl/Nitric	Flux/Argon	420	None	6.3
Sn97/Cu3	HCl/Nitric	Flux/Argon	520	None	5.7
Bi95/Sn5	HCl/Nitric	Flux/Argon	365	non-sphere	

* Solders were prepared by abrasion cleaning

In addition to these studies on simple coupon specimens, mockups of divertor dump plates joined by a compliant layer have been designed and fabricated for electron beam, high-heat-flux testing at the Plasma

Materials Test Facility (PMTF) at Sandia National Laboratories and thermal conductivity studies at UCLA. The PMTF mockups consist of four 10 x 10 cm, finned copper plate sandwiches, each with a 0.2-mm thick solder joint. The UCLA specimens are 2 cm finned disks with the same compliant joint. All mockup parts have been fabricated. The mockups will be pre-wetted with candidate compliant materials on both upper and lower plates. A solder pre-form will then be inserted between the two plates and eight thermocouples installed. The assembly will finally be fired in a braze furnace with a hydrogen background to 400°C. Based on the initial wetting results, In90/Ag10 solder will be used for mockup fabrication. The HHF tests will measure changes in thermal conductivity during the phase transformation between solid and liquid and investigate the effects of thermal cycling on performance including possible void formation and de-wetting. The effects of thermal stress on compliant layer performance will also be investigated. The mechanical integrity of the test specimens and the robustness of the compliant layers will be evaluated under various heat fluxes.

IV. TPE SAMPLE HOLDER DESIGN

The industrial team is also supporting the evaluation of tritium permeation and inventory in plasma facing materials by developing sample holders for the upgraded Tritium Plasma Experiment installation at LANL. Design requirements for the sample holders are summarized in Table 3. The design is complicated by the fact that samples will be subjected to heat fluxes comparable to those in ITER (1-3 MW/m^2) but can only be contacted on 20% of the exposed surface area for cooling. Thermal analyses show that hard contact with the back of the sample is required to reliably achieve the desired sample temperature uniformity over the anticipated range of surface heating.

Table 3. Sample Holder Design Goals/Requirements

Design Parameter	Value
Sample Material	Beryllium
Sample Size	3 Inch Diameter
Sample Electrical Potential	100-300 V
Sample Incident Heat Flux	100-300 W/cm^2
Surface Temperature Range	300-600°C
Radial Temperature Uniformity	±5%
Collimating Aperture Heat Flux	15 W/cm^2
Cooling Contact Limit	20% total area
Coolant	20°C Water, 90 psia

The proposed sample holder design configuration is depicted in Figure 5. Discrete sample temperatures are provided for a given surface heat flux by varying the spacer block thickness and thermal interface conductance between the sample assembly and the cooling plate. The sample holder assembly employs a standard ceramic-break insulator tube for voltage isolation with custom flanges that mate with the aperture, cooling plate and sample assemblies. All coolant and purge gas lines will include similar insulating breaks. The aperture assembly is grounded and therefore has much lower surface heating which is easily handled by the cooled copper collimating plate. The aperture is supported by three stainless-steel struts to allow open access for viewing the sample. Vacuum sealing around the sample is provided by a Helicoflex Delta seal that is rated for temperatures of 550°C to accommodate expected operating conditions.

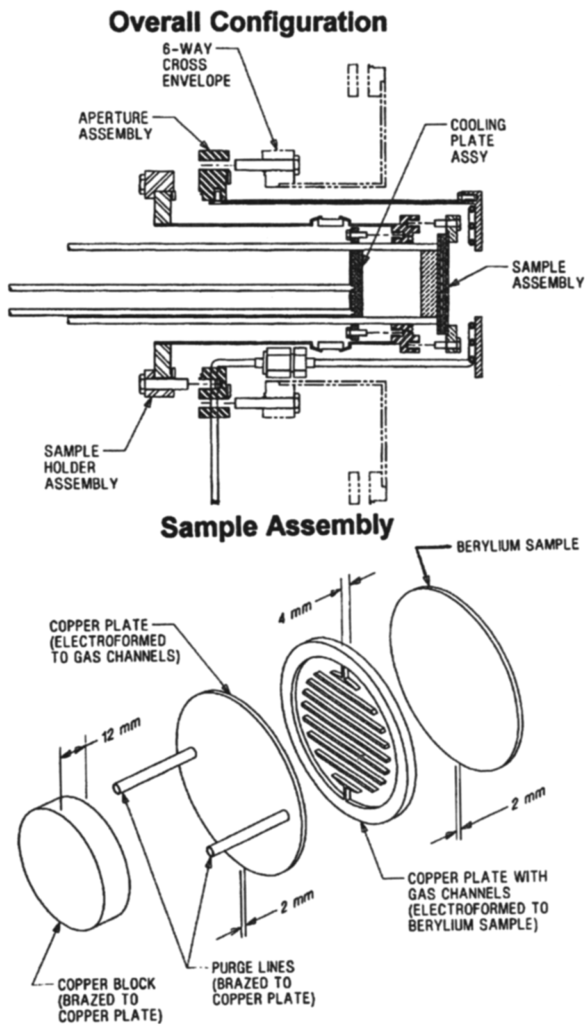

Figure 5. Preliminary sample holder design configuration.

The 20% limit on sample cooling contact necessitates a robust joining process to assure a reliable thermal interface with the sample. Because the experimental objective is characterizing hydrogen diffusion and retention in the sample material, in this case beryllium, there is also a need to minimize the number and thickness of other materials in the permeation path. This makes brazing an unattractive option. Past studies of electroplated copper on beryllium[13,14] have demonstrated bond shear strengths of 250 MPa. In addition, specimens were subjected to five 300°C thermal cycles with no bond strength degradation.

This result, together with the fact that electroplating is a low temperature process that avoids intermetallic formation at the copper-to-beryllium joint, led to its selection for fabricating the sample assembly purge-gas channel structure. The channels will be machined in a 4-mm thick electrodeposited copper layer and the closeout plate will be formed on top as indicated in Figure 5. The purge lines and spacer block are then attached using a quick braze cycle that should not affect the copper-beryllium interface. Another attractive aspect of this approach is that the electroformed copper is expected to provide compliancy by yielding to reduce thermal stress buildup in the sample. This possibility was mentioned in Ref. 14 above where measured shear failure stress increased after thermal cycling. The increase was attributed to work-hardening of the electroformed copper.

Reliable and predictable sample assembly thermal environments are critical to interpreting the test results. Much of the design is therefore driven by the thermal performance requirements. One concern involved the radial temperature uniformity across the sample. Radial uniformity of ±5% is achieved over the 2-inch diameter permeation area, as indicated in Figure 6, by including a 2-mm thick copper layer between the 20% dense purge gas channel structure and the sample. This copper layer enhances hydrogen permeation data interpretation in two ways. First, it provides a barrier to oxide formation on the back surface of the beryllium. Previous studies showed that an oxide layer inhibits surface recombination resulting in an artificial diffusion bottleneck. Diffusion and surface recombination in copper are relatively rapid compared to beryllium thus eliminating this bottleneck. Second, since copper's thermal conductivity is three times that of beryllium, the copper layer sustains most of the radial temperature variation associated with forcing the heat flux through the purge gas channel walls. Temperature gradients in the beryllium are therefore one-dimensional which facilitates interpretation of the experimental results.

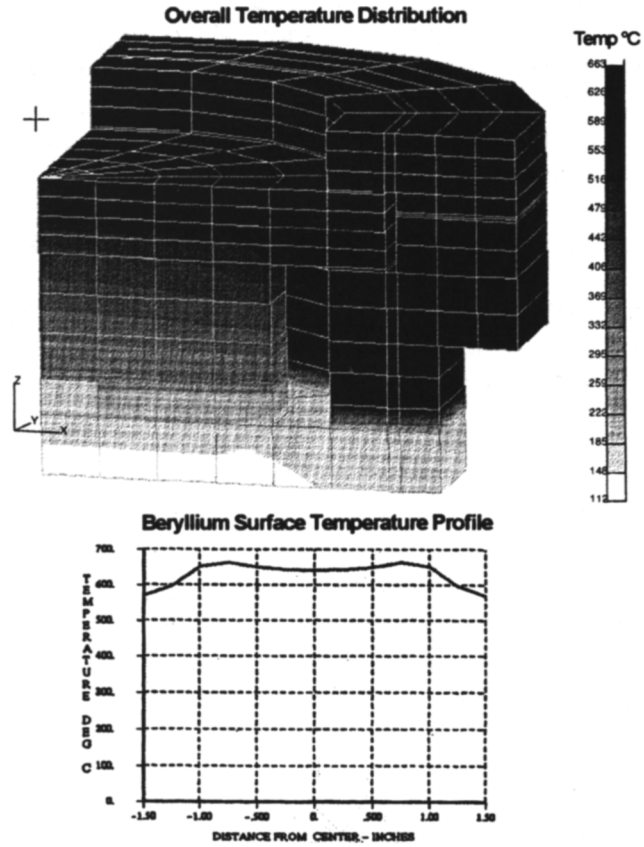

Figure 6. Anticipated temperature distribution in the beryllium sample and sample holder assembly.

Other thermal aspects of the design are illustrated by the sample holder temperature distribution shown in Figure 6. This result is for a 300 W/cm^2 heat flux with a thermal interface conductance of 5.7 W/cm^2-K at the cooling plate. Convection is to 20°C water with a transfer coefficient of 4.0 W/cm^2-K. The cooling plate was designed to handle the peak heat load of 300 W/cm^2 with a maximum wall temperature of 110°C. This is below the bubble formation temperature at atmospheric pressure and, since the bulk fluid is subcooled, should prevent flashover if water pressure is lost. Flanges contacting the sample are thermally isolated from the cooling plate to minimize radial conduction paths that might affect temperature uniformity. Radiation losses were evaluated and found to have negligible effect on temperature uniformity over the 300-600°C sample temperature range of interest.

Attaining the full range of operating temperatures over the factor of three variation in heat flux presented a significant design challenge. The design approach is summarized in Table 4. It depends on the use of spacer blocks and varying thermal interface materials. Brass spacer blocks with grafoil (1.0 W/cm^2-K) and silver-impregnated grease (5.7 W/cm^2-K) interfaces are used to provide discrete operating points at 100 W/cm^2. At higher heat fluxes, operating temperatures are achieved by varying the interface conductance as indicated.

Table 4. Approach for Achieving Desired Sample Operating Temperatures

Heat Flux* (W/cm^2)	Surface Temp (°C)	Hot Interface Temp, Cond (°C, W/cm^2-K)	Cold Interface Temp, Cond (°C, W/cm^2-K)	Spacer Thickness (mm)
100	340	205, 1.0	None	None
	440	305, 1.0	100, 5.7	6, Brass
	540	405, 1.0	100, 5.7	14, Brass
	640	505, 1.0	100, 5.7	22, Brass
200	Lower temperatures not accessible at this heat flux			
	450	None	180, 5.7	None
	540	270, 2.0	None	None
	660	390, 1.0	None	None
300	Lower temperatures not accessible at this heat flux			
	670		265, 5.7	None

* Effective heat flux is factor of 1.26 higher because aperture is enlarged to enhance radial uniformity

V. SUMMARY

The ITER divertor design represents a formidable engineering challenge that is complicated by high-heat fluxes, radiation effects, plasma-compatible materials selection, remote assembly and maintenance operations, and the need for flexibility to adapt to evolving physics requirements. It is encouraging that several alternate materials and configuration options have been identified for the major hardware elements. Ongoing design and technology research and development tasks are working to identify the most attractive (minimal risk yet economic) fabrication approaches for each divertor element. Prototype component fabrication and testing will then validate that processes are scalable to the production status required for final ITER hardware. This will include an early-on emphasis on non-destructive evaluation techniques and remote assembly/maintenance approaches to assure that these important considerations are properly factored into the design.

ACKNOWLEDGMENT

The authors are grateful for the assistance of G. Federici at the ITER co-center in Garching in obtaining recent ITER divertor design drawings.

REFERENCES

1. M.L. Watkins and P-H. Rebut, "Proc. of the 19th European Conf. on Controlled Fusion and Plasma Physics," EPS Conference, Vol. 16C, Part II, 731 (1992).
2. D.E. Driemeyer and J.R. Haines, Editors, "U.S. Design Support Study for the ITER Divertor, Summary Report February-September 1993," ITER/US/93/IV-PF-3 and MDC 93B0544, October 1993.
3. D.B. Heifetz et al., J. Comput. Phys. 46 (1982) 309.
4. M. Petravic, G. Bateman and D. Post, Fourth International Workshop on Plasma Edge Theory in Fusion Devices, Varenna, Italy (1993).
5. J.N. Brooks, D.N. Ruzic, D.B. Hayden, and R.B. Turkot Jr., "Surface Erosion Issues and Analysis for Dissipative Divertors," Presented at the 11th International Conference on Plasma Surface Interactions in Controlled Fusion Devices, May 1994, Mito, Japan. Submitted to J. Nucl. Matl.
6. A. B. Shapiro, "FACET - A Radiation View Factor Computer Code for Axisymmetric, 2D Planer, and 3D Geometries with Shadowing," LLNL, UCID-19887, 1983.
7. H. C. Hottel and A. F. Sarofin, "Radiative Heat Transfer," McGraw-Hill, New York, 1967.
8. J. V. Del Bene, "Computer Code HOTTLF," GA Memo, 1973.
9. C. B. Baxi and H. Falter, "Analytical Prediction of Thermal Performance of Hypervapotron and its Application to ITER," *Fusion Technology*, pp. 186-190, 1992.
10. M. Carelli et al., "A Simpler, Safer, Higher Performance Cooling System Arrangement for Water-Cooled Divertors," these proceedings.
11. G. Federici et al., "Design, Materials and R&D Issues of Innovative Thermal Contact Joints for High Heat Flux Applications," to be presented at the Third International Symposium on Fusion Nuclear Technology, Los Angeles, CA, (1994).
12. G. Federici et al., "Innovative Design and Material Solutions of Thermal Contact Layers for High Heat Flux Applications in Fusion," these proceedings.
13. J.W. Dini and H.R. Johnson, "Joining Beryllium by Plating," *Plating and Surface Finishing*, page 41, June, 1976.
14. L. Jacobson and M. Hill, *Final Report for the Lightweight Materials Program, Oct. 1987 - Dec. 1988*, Los Alamos National Laboratory Report, LAUR-89-2065.